Chemistry–A European Journal

Research Article
doi.org/10.1002/chem.202300610

Chemistry Europe
European Chemical Societies Publishing

www.chemeurj.org

Special Collection

Organometallic–Organic Hybrid Assemblies Featuring the Diantimony Complex $[Cp_2Mo_2(CO)_4(\mu,\eta^2\text{-}Sb_2)]$, Ag^I Ions and N-Donor Molecules as Building Blocks

Pavel A. Shelyganov,[a] Mehdi Elsayed Moussa,[a] Michael Seidl,[a, b] and Manfred Scheer*[a]

Dedicated to Professor Kurt Merzweiler on the occasion of his 65th birthday

Abstract: The reactions of the organometallic ligand complex $[Cp_2Mo_2(CO)_4(\mu,\eta^2\text{-}Sb_2)]$ (**C**) with Ag[TEF] ($[TEF]^- = [Al\{OC(CF_3)_3\}_4]^-$) in the presence of a number of di- or polytopic N-donor molecules (1,6,7,12-tetraazaperylene (**L1**), 2,2′-bipyrimidine (**L2**), 4,4′-bipyridine (**L3**), trans-1,2-di(4-pyridyl)ethylene (**L4**) and 1,3-di(4-pyridyl)propane (**L5**)), were studied. Depending on the reaction stoichiometry and choice of linker, these reactions lead to the selective formation of dimeric or tetrameric supramolecular coordination complexes as well as 1D and 2D coordination polymers (CPs). The presented compounds are unique examples of supramolecular complexes incorporating both organometallic Sb-donor and organic N-donor molecules as ligands to stabilize metal ions. Moreover, one of the formed compounds, the CP $[Ag_4(\eta^{2:1}\text{-}\mathbf{C})_4(\mathbf{L4})_4]_n[TEF]_{4n}$, represents an exceptional 1D polymer incorporating both N- and Sb-donor ligands as connectors for metal ions.

Introduction

The use of metal-directed self-assembly for the construction of well-defined solid-state structures has attracted significant attention during the past few decades.[1] In particular, Ag^I-based supramolecular compounds have been captivating targets due to their vast structural diversity[2] and antimicrobial properties[3] rendering them promising candidates for medical applications.[4] One reason for such a structural diversity is that Ag^I ions readily coordinate organic ligands featuring a large variety of donor atoms (commonly N-, O-, S- or P- as well as less common Se-, C- and As-donor atoms).[2,4d,5] Another reason is the flexibility of the coordination sphere of the Ag^I ion (linear, trigonal planar, tetrahedral, square-planar, trigonal bipyramidal, and other geometries are known).[5a,g–i] However, such flexibility often challenges the directionality of the assembling processes towards the selective formation of targeted products.[6] To increase the selectivity of such reactions, several methods were developed.[7] A common strategy is based on connecting Ag^I ions by rigid di- or polytopic organic ligands which, due to their limited conformational freedom, usually directs aggregation reactions towards the selective formation of only one product.[5i,8]

In contrast to organic ligands, organometallic complexes are limitedly used as connectors for Ag^I ions.[9] Due to the lack of such examples in this field, our group focuses on using organometallic polyphosphorus (P_n, $n = 2–6$)[10] and polyarsenic (As_n, $n = 2, 3, 5$)[11] ligand complexes with flexible coordination modes as connectors between Ag^I and other metal ions (two-component reactions). This approach afforded a vast diversity of novel supramolecular aggregates including discrete (supramolecular coordination complexes (SCCs),[10e,11–12] inorganic fullerene-like nanospheres,[10b,13] nanosized capsules[14] and bowls[15]) as well as extended (1D, 2D and 3D coordination polymers (CPs)) assemblies.[10a,c,f,12c,16] Furthermore, we were interested in investigating reactions of these organometallic complexes with metal ions in the presence of di- or polytopic organic N-donor molecules (three-component reactions). These more complex reactions allowed for the formation of an unprecedented class of hybrid polymers in which both organic molecules and organometallic ligand complexes are found to link metal centers.[8a,17]

Two of the simplest organometallic building blocks in this field are the dipnictogen complexes $[Cp_2Mo_2(CO)_4(\mu,\eta^2\text{-}E_2)]$ (E = P (**A**);[18] As (**B**),[19] $Cp = C_5H_5$). In the last two decades, the supramolecular chemistry of these compounds has been intensively studied due to their relatively low air sensitivity and ease of accessibility at gram scale. Very recently, we became interested in extending our research towards the diantimony

[a] P. A. Shelyganov, Dr. M. Elsayed Moussa, Dr. M. Seidl, Prof. Dr. M. Scheer
Institute of Inorganic Chemistry, University of Regensburg
93040 Regensburg (Germany)
E-mail: manfred.scheer@chemie.uni-regensburg.de
Homepage: http://www.uni-regensburg.de/chemie-pharmazie/anorganische-chemie-scheer

[b] Dr. M. Seidl
Institut für Allgemeine, Anorganische und Theoretische Chemie
Universität Innsbruck, Centrum für Chemie und Biomedizin (CCB)
Innrain 80–82, 6020 Innsbruck (Austria).

Supporting information for this article is available on the WWW under https://doi.org/10.1002/chem.202300610

Special Collection Part of a Special Collection on the p-block elements.

complex $[Cp_2Mo_2(CO)_4(\mu,\eta^2\text{-}Sb_2)]$ (**C**), the heavier analog of **A** and **B**. As opposed to **A** and **B**, complex **C** is readily oxidized in the presence of air as well as, under specific reaction conditions, by Ag^I salts.[20] Nevertheless, by carefully tuning the reaction conditions, we were finally able to isolate a large variety of unprecedented SCCs with unique solid-state features from two-component reactions involving **C** with a range of Ag^I salts.[20a] This achievement paved the way for the investigation of three-component reactions of **C**, Ag^I ions and multitopic N-donor organic molecules aimed at the synthesis of unprecedented hybrid organometallic–organic aggregates. Herein, we report the reactions of **C** with Ag[TEF] ($[TEF]^- = [Al\{OC(CF_3)_3\}_4]^-$) in the presence of variable rigid (except for the somewhat flexible molecule **L5**, see below) organic N-donor molecules (1,6,7,12-tetraazaperylene (**L1**), 2,2′-bipyrimidine (**L2**), 4,4′-bipyridine (**L3**), *trans*-1,2-di(4-pyridyl)ethylene (**L4**) and 1,3-di(4-pyridyl)propane (**L5**)). Depending on the choice of linker and the reaction stoichiometry, these reactions allow the selective formation of organometallic–organic hybrid aggregates including the dimer $[(\eta^2\text{-}\mathbf{C})_4Ag_2(\mathbf{L1})][TEF]_2$ (**1**), the tetramer $[(\eta^2\text{-}\mathbf{C})_6Ag_4(\mathbf{L2})_3][TEF]_4$ (**3**), the 1D CPs $[(\eta^2\text{-}\mathbf{C})Ag(\mathbf{L1})]_n[TEF]_n$ (**2**), $[(\mu,\eta^{2:1}\text{-}\mathbf{C})_4Ag_4(\mathbf{L4})_4]_n[TEF]_{4n}$ (**5**) and $[(\eta^2\text{-}\mathbf{C})_2Ag_2(\mathbf{L5})_3]_n[TEF]_{2n}$ (**6**) and the 2D CP $[(\eta^2\text{-}\mathbf{C})Ag(\mathbf{L3})_{1.5}]_n[TEF]_n$ (**4**). Some Ag^I coordination complexes possessing both N-donor linkers and simple organic Sb-donor ligands (though limited to $SbPh_3$ and $(SbPh_2)_2CH_2$) were previously reported.[21] However, to the best of our knowledge, no organometallic compounds featuring Sb-donor atoms together with organic N-donor molecules have been used to coordinate Lewis acidic metal ions. Moreover, the CP **5** is a unique example in which both N- and Sb-donor polytopic molecules are used to connect metal centers.

Results and Discussion

In the ESI-MS spectra of solutions of the aforementioned two-component reactions of **C** with Ag[TEF] (**C**:Ag[TEF] ratios of 3:1, 2:1 and 1:1 were examined), the most abundant peak was observed to correspond to the monocationic species $[\mathbf{C}_2Ag]^+$ (Scheme 1a),[20a] leading to the question as to whether the silver ions in these solutions are accessible by additional N-donor organic molecules, which would allow for the formation of mixed supramolecular compounds.

In a first approach, ligand **L1** featuring a chelating bis(α-diimine) moiety was selected. The reactions of **C** with Ag[TEF] were performed using a 3:1 or 2:1 molar ratio in the presence of one or two equivalents of **L1** in CH_2Cl_2 at room temperature. These reactions led, upon slow diffusion of *n*-pentane, to the selective formation of SCC $[(\eta^2\text{-}\mathbf{C})_4Ag_2(\mu,\eta^{1:1:1:1}\text{-}\mathbf{L1})][TEF]$ (**1**) and 1D organometallic–organic CP $[\{\eta^2\text{-}\mathbf{C})Ag(\mu_2,\eta^{1:1:1:1}\text{-}\mathbf{L1})]_n[TEF]_n$ (**2**) as dark brown crystals in good yields (76 and 64%, respectively) suitable for X-ray diffraction analysis (Scheme 1a). The crystal structure of **1** reveals a bimetallic supramolecular complex consisting of two $[(\eta^2\text{-}\mathbf{C})_2Ag]$ organometallic nodes connected to each other by one bridging molecule of **L1** (Scheme 1b). Thus, **1** can be seen as a product of the coordination of one molecule of **L1** to two $[\mathbf{C}_2Ag]^+$ species each via one of its α-diimine functions. The thermodynamic feasibility of this transformation in CH_2Cl_2 was confirmed by DFT calculations which show a both strongly exothermic ($\Delta H = -235.6\ kJ\cdot mol^{-1}$) and strongly exergonic ($\Delta G = -130.4\ kJ\cdot mol^{-1}$) character (ωB97XD/def2-SVP level of theory with PCM solvent model (for more details see the Supporting Information (Figure S20, Table S4)). Each Ag^I ion in **1** is hexacoordinated by four Sb and two N atoms, thus possessing a distorted trigonal prismatic environment. The solid-state structure of **2** shows a 1D CP consisting of organometallic $[(\eta^2\text{-}\mathbf{C})Ag]$ nodes instead of $[(\eta^2\text{-}\mathbf{C})_2Ag]$ nodes as

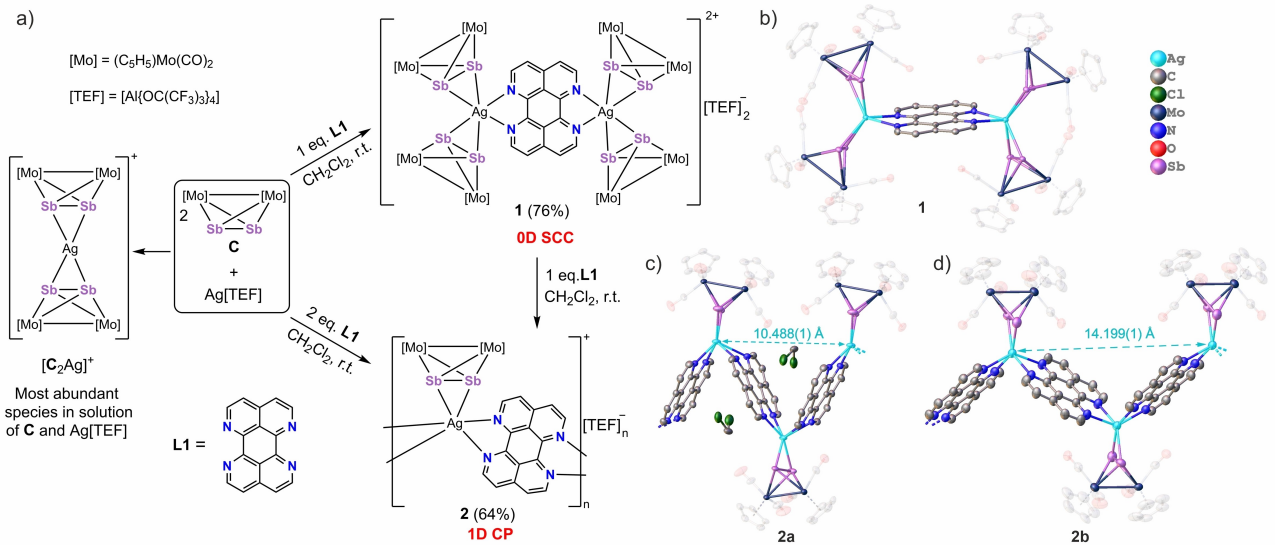

Scheme 1. Summary of the reactions between **C** and Ag[TEF] in the presence of **L1**. a) Synthesis of **1** and **2** (yields are given in parentheses) and most abundant cationic species in solution of **C** and Ag[TEF]. b) Solid-state structure of SCC **1** and c) and d) sections of the two polymorphs of the CP **2**, **2a** (crystallized form CH_2Cl_2) and **2b** (crystallized from *o*-DFB). Anions and H atoms are omitted for clarity; Cp and CO ligands are faded out.

present in **1**. Each two adjacent nodes in **2** are linked together via one ligand **L1** to the polycationic chain. Accordingly, **2** is presumably formed from $[\mathbf{C}_2\mathrm{Ag}]^+$ by coordination of one linker **L1** to two $[\mathbf{C}_2\mathrm{Ag}]^+$ moieties (akin to **1**) together with the substitution of one complex **C** from each $[\mathbf{C}_2\mathrm{Ag}]^+$ unit by one α-diimine function of another linker **L1**. Similar to **1**, the formation of **2** from $[\mathbf{C}_2\mathrm{Ag}]^+$ and **L1** in CH_2Cl_2 was calculated to be notably exothermic ($\Delta H = -110.1$ kJ·mol^{-1}) and exergonic ($\Delta G = -76.4$ kJ·mol^{-1}).[22] Interestingly, compound **2** can be crystallized from two different solvents (CH_2Cl_2 and *o*-$C_6H_4F_2$ (*o*-DFB)). As a result, two different polymorphs of **2** were selectively isolated with the major difference referring to the angle between two molecules of **L1** at the Ag^{I} center (defined as angle Ψ between the normals of the mean planes of **L1** molecules, Scheme 1c, d). The compound crystallized from CH_2Cl_2 (**2a**, Scheme 1c) shows a smaller Ψ (51.41(1)°), while in the other polymorph obtained from *o*-DFB (**2b**, Scheme 1d) Ψ is almost twice as big (98.21(1)°) as **2a**.

Additionally, due to differing angles Ψ, the 1D chain in **2a** is more compact while, in **2b**, it is more expanded (interatomic distances between second-closest Ag^{I} centers are 10.488(1) Å and 14.199(1) Å, respectively). In **2a**, the voids formed by a zig-zag-shaped polymeric chain are each partially occupied by one CH_2Cl_2 molecule, while the voids of **2b** are partially occupied by *o*-DFB solvent molecules as well as $[TEF]^-$ anions which is likely to be the main reason for the expansion of the polymeric chain in **2b**. Remarkably, CP **2** can be theoretically obtained from **1** by a formal substitution of one ligand **C** by a molecule of **L1** in each of the $[(\eta^2\text{-}\mathbf{C})_2\mathrm{Ag}]$ fragments. To examine if this transformation is experimentally feasible, **1** was dissolved in CH_2Cl_2 and reacted with another equivalent of **L1** which indeed afforded the selective formation of **2** (specifically **2a** since CH_2Cl_2 was used as a solvent, Scheme 1a). According to the abovementioned calculations, this transformation is somewhat endothermic ($\Delta H = 13.8$ kJ·mol^{-1}) and very slightly endergonic ($\Delta G = 3.8$ kJ·mol^{-1}) (for more details see the Supporting Information). Provided that the Gibbs free energy difference is very small, it is not surprising that such a very slightly uphill reaction does proceed.

The isolation of **1** and **2** proves the possibility to obtain both discrete and polymeric organometallic–organic aggregates in a controlled, stepwise fashion by one-pot three-component self-assembly reactions. Moreover, according to the CSD database,[23] **1** and **2** are the first reported examples of compounds containing transition metal centers coordinated to four Sb- and two N-atoms or two Sb- and four N-atoms, respectively.

As a second step, reactions of **C** with Ag[TEF] (3:1 and 2:1 ratio) in the presence of **L2** were studied. The 2:1 ratio reaction followed by slow diffusion of *n*-pentane at −30 °C led to the formation of complex $[(\eta^2\text{-}\mathbf{C})_6\mathrm{Ag}_4(\mu,\eta^{1:1:1:1}\text{-}\mathbf{L2})_3][TEF]_4$ (**3**) as red crystalline material in moderate isolated yields (45%; Scheme 2a). X-ray diffraction analysis reveals that **3** consists of four organometallic nodes connected to each other via three **L2** linkers. The two terminal nodes are each composed of an Ag^{I} ion capped by two complexes **C**, while the two central ones are each composed of an Ag^{I} ion capped by one complex **C** (Scheme 2b). Compound **3** is probably formed from $[\mathbf{C}_2\mathrm{Ag}]^+$ species and **L2** via steps similar to those assumed for the formation of **1** and **2** (see above). Remarkably, DFT calculations suggest that the formation of both nodes $[(\eta^2\text{-}\mathbf{C})_2\mathrm{Ag}(\mu,\eta^{1:1}\text{-}\mathbf{L2})]^+$ ($\Delta H = -115.2$ kJ·mol^{-1}, $\Delta G = -60.5$ kJ·mol^{-1}) and $[(\eta^2\text{-}\mathbf{C})\mathrm{Ag}(\mu,\eta^{1:1}\text{-}\mathbf{L2})_2]^+$ ($\Delta H = -103.2$ kJ·mol^{-1}, $\Delta G = -52.1$ kJ·mol^{-1}) from species $[\mathbf{C}_2\mathrm{Ag}]^+$ and **L2** are thermodynamically feasible (for more details see the Supporting Information). All Ag^{I} ions in **3** possess a distorted trigonal prismatic geometry. After coordinating the necessary number of molecules **L2**, each of the two types of organometallic nodes present in **3** alone could potentially form either dimeric or 1D polymeric species (along the lines of the **L1**-containing complexes **1** and **2**, respectively). Accordingly, oligomer **3** can be formally seen as an intermediate stage between the dimeric SCC and the polymeric CP

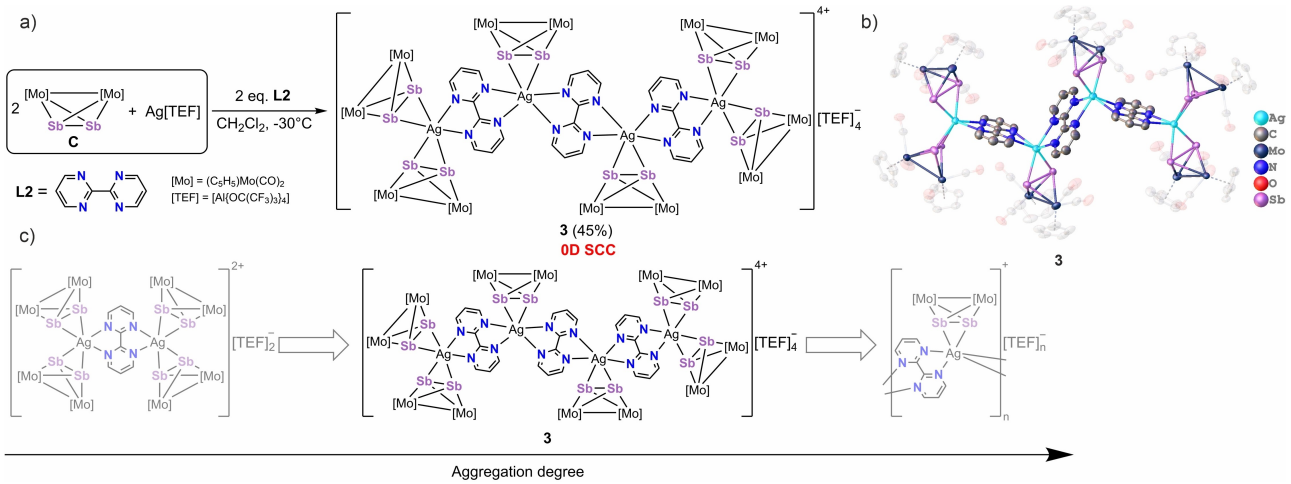

Scheme 2. Summary of the one-pot reaction between **C** and Ag[TEF] in the presence of **L2**. a) Synthesis of **3**; the yield is given in parentheses. b) Solid-state structure of SCC **3**. Anions and H atoms are omitted for clarity; Cp and CO ligands are faded out. c) Comparison of **3** with hypothetical "limitedly aggregated" dimeric and "infinitely aggregated" polymeric species. The hypothetical species are shown as faded out.

(Scheme 2c; however, neither postulated compound could be isolated experimentally).

The isolation of **1**–**3** provoked the question of whether using pyridine-based molecules (ditopic N-donor molecules) instead of the ligands **L1** and **L2** (tetratopic N-donor molecules) would allow the coordination of more ligands on the Ag^{I} ions favoring the formation of CPs of higher dimensionality. Accordingly, the ditopic pyridine-based linkers **L3**–**L5** were selected to probe three-component reactions with **C** and Ag^{I} ions. The reactions were carried out with 3:1, 2:1 and 1:1 ratios of **C**:Ag^{I} in the presence of the ligands **L3**–**L5**. The addition of two equivalents of **L3**–**L5** to the stirred reaction mixture of **C** and Ag[TEF] in the C:Ag^{I} ratio of 1:1 in CH_2Cl_2 followed by its layering with *n*-pentane at −30 °C selectively yielded the organometallic–organic hybrid CPs $[(\eta^2\text{-}\mathbf{C})Ag(\mu,\eta^{1:1}\text{-}\mathbf{L3})_{1.5}]_n[TEF]_n$ (**4**, 23% yield), $[(\mu,\eta^{2:1}\text{-}\mathbf{C})_4Ag_4(\mu,\eta^{1:1}\text{-}\mathbf{L4})_4]_n[TEF]_{4n}$ (**5**, 53% yield) and $[(\eta^2\text{-}\mathbf{C})_2Ag_2(\mu,\eta^{1:1}\text{-}\mathbf{L5})_3]_n[TEF]_{2n}$ (**6**, 63% yield) as orange crystals in moderate to good yields (Scheme 3a).

The crystal structure of **4** shows a 2D CP consisting of organometallic $[(\eta^2\text{-}\mathbf{C})Ag]$ nodes connected each to three neighboring nodes by rigid pillar-like linkers **L3**. The $[(\eta^2\text{-}\mathbf{C})Ag]$ units form the vertices of the 2D honeycomb network of the hcb topology (Scheme 3c) with the cavities of the meshes having hexagonal shapes of a maximum dimension of approximately 1.7 nm.[24] These cavities are occupied by $[TEF]^-$ anions. Remarkably, both the structure and the topology of **4** are in line with those of CP assembled from diarsenic complex **B**, Ag^{I} ions and ligand **L3**.[12a]

The solid-state structure of **5** reveals a 1D CP with a ladder-like structure. The repeating units of **5** consist of four Ag^{I} ions, each of which are bridged pairwise by two complexes **C** possessing a bridging $\eta^{2:1}$-coordination mode. Together with two linkers **L4**, two of the bimetallic fragments $[(\mu,\eta^{2:1}\mathbf{C})_2Ag_2]$ form a metallaparacyclophane-like metallocycle $[(\mu,\eta^{2:1}\mathbf{C})_4Ag_4(\mu,\eta^{1:1}\text{-}\mathbf{L4})_2]$ (Scheme 3d). Remarkably, the Ag···Ag interatomic distance in this fragment is 3.543(8)–3.655(6) Å which is longer than the sum of the van der Waals radii of two Ag ions (3.44 Å),[25] suggesting the absence of argentophilic interactions. Notably, the pyridine rings of the **L4** molecules in this metallocycle are parallel-displaced (fold angle 3.7(4)°) and located only 3.728(6) Å apart which is close to the distance reported by Sherrill et al. for a calculated parallel-displaced pyridine dimer (3.848 Å) featuring π–π stacking interactions.[26] Metallocycles $[(\mu,\eta^{2:1}\mathbf{C})_4Ag_4(\mu,\eta1:1\text{-}\mathbf{L4})_2]$ are further connected to each other through two more linkers **L4** building the 1D polymeric network. The cavities of the meshes in **5** have a rhombic shape with a maximal dimension of approximately 1.8 nm.[24] Similar to **4**, the cavities are filled with $[TEF]^-$ anions. To the best of our knowledge, **5** is the first and only example in which both Sb- and N-donor molecules are used as linkers to connect metal ions in one compound. The solid-state structure analysis of **6** reveals a 1D CP in which bimetallic metallocycles $[(\eta^2\text{-}\mathbf{C})_2Ag_2(\mu,\eta^{1:1}\text{-}\mathbf{L5})_2]$ are connected to each other by linkers **L5** into an infinite 1D assembly (Scheme 3b). Each metallocycle in **6** contains two $[Ag(\eta^2\text{-}\mathbf{C})]$ nodes linked by two ligands **L5**. The convergence of two ligands **L5** (bending in such a way that N atoms of two linkers **L5** coordinate pairwise two Ag^{I} ions), which is a prerequisite for the formation of the metallocycle $[(\eta^2\text{-}\mathbf{C})_2Ag_2(\mu,\eta^{1:1}\text{-}\mathbf{L5})_2]$, is feasible due to the somewhat flexible backbone of **L5** providing enough conformational freedom.

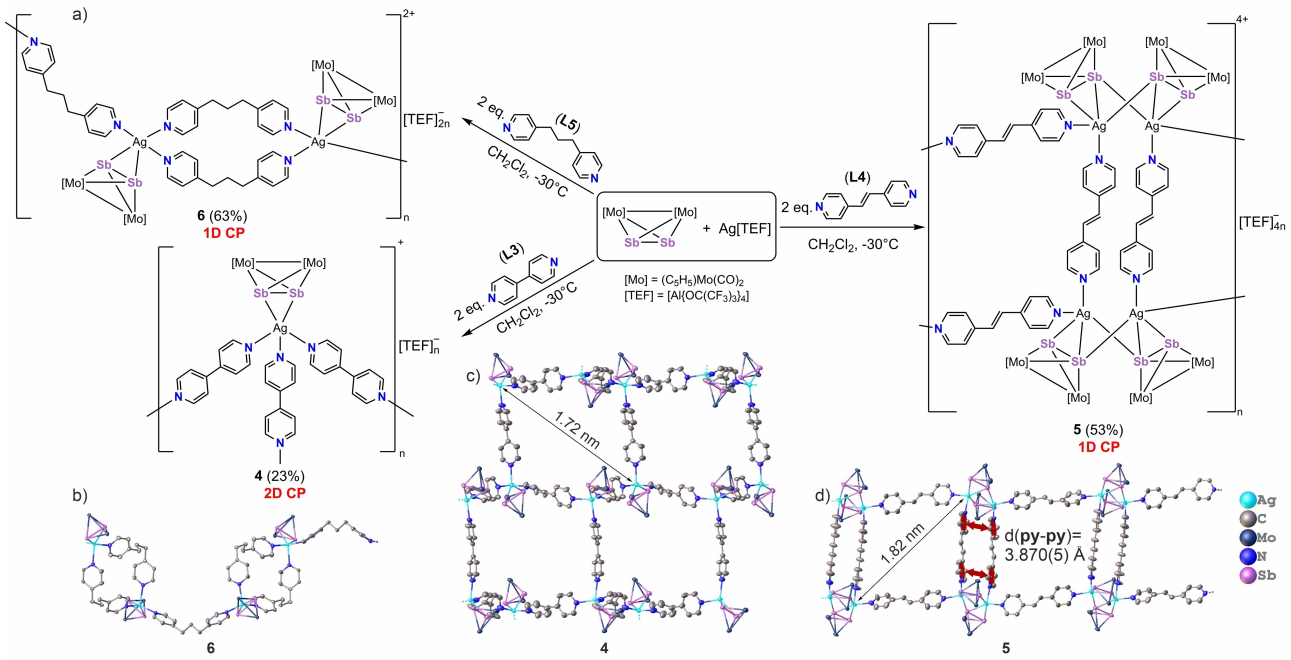

Scheme 3. Summary of the one-pot reaction between **C** and Ag[TEF] in the presence of pyridine-based linkers **L3**-**L5**. a) Synthesis of CPs **4**–**6**; yields are given in parentheses. Sections of b) 1D CP **6**, c) 2D CP **4** and d) 1D CP **5**. Anions, hydrogen atoms as well as Cp and CO ligands are omitted for clarity. Neighboring pyridine rings presumably presenting π–π stacking interactions are highlighted in red. py = C_5H_5N.

Interestingly, in both **6** and **4**, the Ag^{I} ion coordinates, in addition to two Sb-atoms of complex **C**, to three N-atoms from the pyridine linkers. However, contrary to **6**, the rigid linkers **L3** in **4** promote a divergent geometry disfavoring the formation of a metallocycle similar to that observed in **6**, consequently directing the reaction towards the formation of a CP of a higher dimensionality. DFT calculations imitating the formation of CPs **4**–**6** from $[\mathbf{C}_2Ag]^+$ predict these reactions to be both exothermic ($\Delta H = -100.9$ kJ·mol^{-1} (**4**, **6**), -198.0 kJ·mol^{-1} (**5**)) and exergonic ($\Delta G = -14.5$ kJ·mol^{-1} (**4**, **6**), -42.1 kJ·mol^{-1} (**5**)) (for more details see the Supporting Information).[27] Each Ag^{I} ion in **4**–**6** is pentacoordinated by two Sb-atoms and three N-atoms (**4** and **6**) or three Sb- and two N-atoms (**5**). This is in contrast to the hexacoordinated Ag^{I} ions found in **1**–**3**. The possible rationalization is the steric bulk created by the backbone built of pyridine rings preventing the Ag^{I} ions from coordinating the sixth donor atom. The coordination geometry of the Ag^{I} centers in **4** is best described as a distorted trigonal bipyramid, while, in **5**, it is closer to a distorted tetragonal pyramid.[28] Interestingly, in **6**, one of the Ag^{I} centers possesses a distorted trigonal pyramidal coordination sphere while the other one is closer to a distorted tetragonal pyramid (see the Supporting Information for details). These differences in the coordination geometries of the Ag^{I} centers in **4**–**6** are not surprising due to the flexible and adaptive coordination sphere of Ag^{I} ions in general.

The Sb–Sb bond lengths in **1**–**6** (2.736(3)–2.806(6) Å) are slightly elongated as compared to those in the non-coordinated ligand complex **C** (2.687(1) Å)[29] and comparable to those in two-component SCCs of Ag[TEF] and **C** (2.722(1)–2.778(1) Å).[20a] The Ag–Sb bond lengths in **1**–**6** (2.713(8)–2.993(1) Å) are also comparable to those in the two-component SCCs of Ag[TEF] and **C** (2.768(1)–3.148(1) Å).[20a]

Compounds **1**–**6** are well soluble in common organic solvents such as CH_2Cl_2 and CH_3CN, slightly soluble in THF and C_6H_6 and insoluble in *n*-pentane. The room temperature ^{1}H NMR spectra of **1**–**6** in CD_2Cl_2 show each one sharp singlet in the range of 5.14-5.25 ppm corresponding to the Cp protons of the ligand complex **C** as well as characteristic signals for organic linkers **L1**–**L5** (see the Supporting Information for details). The signals for the Cp rings in **1**–**6** are slightly downfield shifted as compared to that observed in the ^{1}H NMR spectrum of the non-coordinated complex **C** (5.10 in CD_2Cl_2).[20a] The positive ESI-MS spectra of **1** and **2** in CH_2Cl_2 show together with the most abundant peak attributable to the fragment $[Ag\mathbf{C}(\mathbf{L1})]^+$ peaks corresponding to the fragments $[Ag\mathbf{C}_2]^+$ (76% (**1**), 6% (**2**)), $[Ag_2\mathbf{C}_2(\mathbf{L1})]^{2+}$ (2% (**1**), 38% (**2**)) and $[\{Ag_2\mathbf{C}_2(\mathbf{L1})\}\{TEF\}]^+$ (0.3% (**1**), 0.4% (**2**)). In addition, the ESI-MS spectra indicate the presence of the fragment $[Ag\mathbf{C}_2(\mathbf{L1})]^+$ in the solution of **1** but not in that of **2**. These observations reveal an only partial disassembly of the aggregates **1** and **2** in solution. Remarkably, in the ESI-MS spectra of **3**, the main peaks correspond to the fragments $[Ag\mathbf{C}(\mathbf{L2})]^+$ (100%) and $[Ag\mathbf{C}_2]^+$ (65%) while larger fragments such as $[\{Ag_2\mathbf{C}_2\}\{Cl\}]^+$ (0.3%), $[\{Ag_2\mathbf{C}_3\}\{Cl\}]^+$ (0.1%) and $[\{Ag_2\mathbf{C}_2(\mathbf{L2})\}\{TEF\}]^+$ (0.1%) with more than one silver ion only correspond to very minor peaks. Finally, the ESI-MS spectra of solutions of **4**–**6** show together with the main fragment $[Ag\mathbf{C}_2]^+$ also the moieties $[Ag\mathbf{C}(\mathbf{L})]^+$ (**L** = **L3** (**4**, 45%), **L4** (**5**, 51%), **L5** (**6**, 34%)). The solid-state IR spectra of compounds **1**–**6** reveal two to three strong broad absorptions between 1893 and about 1956 cm^{-1} corresponding to the stretching vibrations of the carbonyl ligands of the coordinated complexes **C**. These vibrations appear at higher energies as compared to those reported for the non-coordinated complex **C** (1880 and 1916 cm^{-1}).[20a]

Conclusion

In summary, we have demonstrated that three-component reactions of the diantimony complex $[Cp_2Mo_2(CO)_4(\eta^2\text{-}Sb_2)]$ (**C**) with Ag[TEF] in the presence of N-donor linkers afforded a number of new, discrete (**1**, **3**) and polymeric (**2**, **4**–**6**) organometallic–organic hybrid assemblies. The solid-state structures of **1** and **3** show di- and tetrameric 0D SCCs, respectively. The assemblies **2**, **5**–**6** are 1D CPs, and **4** represents a 2D CP. To the best of our knowledge, compounds **1**–**6** are the first and only examples of compounds in which organometallic Sb- and organic N-donor molecules are co-used as building blocks to coordinate metal ions. Moreover, **5** represents a unique example in which both polytopic Sb- and N-donor molecules are used as connectors between metal ions. These results show that, despite the challenges associated with the ease of the oxidation of **C** with Ag^{I} ions, we were able to isolate a variety of new original supramolecular assemblies by using **C** as a building block; this is an enormous enrichment of the research field of transition metal compounds bearing naked pnictogen atoms. Our current investigations in this field focus on extending this approach to the even more oxidative-sensitive dibismuth complex $[Cp_2Mo_2(CO)_4(\eta^2\text{-}Bi_2)]$ as well as to heterodiatomic dipnictogen complexes $[Cp_2Mo_2(CO)_4(\eta^2\text{-}EE')]$ (E = Sb, Bi, E' = As, Sb) as connectors in the supramolecular chemistry of metal ions.

Experimental Section

Apparatus, materials and methods: All manipulations were performed under an atmosphere of dry nitrogen using standard glove box and Schlenk techniques. All solvents were purified by standard procedures. The compounds $[Cp_2Mo_2(CO)_4(\mu,\eta^2\text{-}Sb_2)]$ (**C**),[30] $Ag[Al\{OC(CF_3)_3\}_4]$ (Ag[TEF]),[31] and 1,6,7,12-tetraazaperylene (**L1**)[32] were prepared according to literature procedures. Other chemicals were obtained from TCI (1,3-di(4-pyridyl)propane (**L5**)), Sigma Aldrich (4,4′-bipyridine (**L3**), *trans*-1,2-di(4-pyridyl)ethylene (**L4**)) (now Merck) or Alfa Aesar (2,2′-bipyrimidine (**L2**)). All yields are reported with respect to Ag[TEF]. The NMR spectra were recorded on an Bruker Avance III HD 400 spectrometer (^{1}H: 400 MHz, $^{13}C\{^1H\}$: 100 MHz, $^{19}F\{^1H\}$: 376 MHz) with δ (ppm) referenced to external standards $SiMe_4$ (^{1}H, $^{13}C\{^1H\}$), $CFCl_3$ ($^{19}F\{^1H\}$) (**1**-**6**). IR spectra were recorded on a ThermoFisher Nicolet iS5 FTIR spectrometer with KBr carrier phase (**1**-**6**). Mass spectra were recorded on an Agilent Q-TOF 6540 UHD spectrometer (**1**-**6**). C, H, N analyses were measured on an Elementar Vario EL III apparatus (**1**-**6**) and were carried out repeatedly. Single crystals were measured on a XtaLAB SynergyR DW diffractometer equipped with an HyPix-Arc 150 detector (**1**, **2a**, **2b**, **3**, **4**) or on a SuperNova Dualflex diffractometer equipped with an Atlas^{S2} CCD detector (**5**, **6**).

Experimental details

*Synthesis of [(η^2-C)$_4$Ag$_2$(μ,$\eta^{1:1:1:1}$-L1)][TEF]$_2$ (**1**)*: A solution of Ag[TEF]·CH_2Cl_2 (23 mg, 0.02 mmol, 1 equiv.) in CH_2Cl_2 (4 mL) was added to a solution of **C** (27 mg, 0.04 mmol, 2 equiv.) in CH_2Cl_2 (4 mL) at room temperature. After stirring for 20 min, a solution of **L1** (5.1 mg, 0.02 mmol, 1 equiv.) in CH_2Cl_2 (3 mL) was added to the reaction mixture. After stirring for 30 min, the clear solution was layered with 30 mL of *n*-pentane. The Schlenk flask was kept in the dark at room temperature and **1** precipitated as brown crystalline material after one week. The product was filtered, washed with *n*-pentane, and then dried in vacuo. Yield: 39 mg (76%). ^{1}H NMR (CD_2Cl_2, 25 °C): δ = 5.14 (s, 40H, H_{Cp}), 8.08 (d, 4H, $^3J_{H,H}$ = 5.8 Hz, H_a), 9.22 (d, 4H, $^3J_{H,H}$ = 5.8 Hz, H_b). ^{13}C{^{1}H} NMR (CD_2Cl_2, 25 °C): δ = 83.8 (s, C_{Cp}), 223.7 (s, C_{CO}). C_a and C_b were not detected due to low intensity of corresponding signals and relatively low concentration of solutions. ^{19}F{^{1}H} NMR (CD_2Cl_2, 25 °C): δ = −75.6 (s, [TEF]$^-$). IR (KBr): $\tilde{\nu}$ = 2924 (w), 1956 (s, CO), 1913 (s, CO), 1735 (w), 1719 (w), 1699 (w) 1686 (w), 1654 (w), 1638 (w), 1604 (w), 1561 (w), 1543 (w), 1524 (w), 1510 (w), 1460 (w), 1421 (w), 1386 (m), 1355 (m) 1303 (s), 1279 (s), 1243(s), 1221 (s), 1166 (m), 1043 (w), 974 (s), 864 (m), 827 (m), 729 (s). ESI-MS (CH_2Cl_2): positive mode: *m/z* 1042.7 (100%, [{$Cp_2(CO)_4Mo_2Sb_2$}Ag($C_{16}H_8N_4$)]$^+$), 1464.3 (76%, [{$Cp_2(CO)_4Mo_2Sb_2$}$_2$Ag]$^+$), 913.6 (2%, [{$Cp_2(CO)_4Mo_2Sb_2$}$_2$Ag$_2$($C_{16}H_8N_4$)]$^{2+}$), 1719.2 (0.5%, [{$Cp_2(CO)_4Mo_2Sb_2$}$_2$Ag($C_{16}H_8N_4$)]$^+$), 2796.1 (0.3%, [{{$Cp_2(CO)_4Mo_2Sb_2$}$_2$Ag$_2$($C_{16}H_8N_4$)}{Al{OC(CF_3)$_3$}$_4$}]$^+$). ESI-MS (CH_2Cl_2): negative mode: *m/z* 966.9 (100%, [Al{OC(CF_3)$_3$}$_4$]$^-$). Elemental analysis (%) calcd for $C_{104}H_{48}Ag_2Al_2F_{72}Mo_8N_4O_{24}Sb_8$ (**1**) (5116.81 g·mol^{-1}): C 24.41, H 0.95, N 1.09; found: C 24.34, H 0.59, N 1.14.

*Synthesis of [(η^2-C)Ag(μ,$\eta^{1:1:1:1}$-L1)]$_n$[TEF]$_n$ (**2**)*: Compound **2** can be synthesized according to two different methods. Method 1: a solution of Ag[TEF]·CH_2Cl_2 (23 mg, 0.02 mmol, 1 equiv.) in CH_2Cl_2 (4 mL) was added to a solution of **C** (27 mg, 0.04 mmol, 2 equiv.) in CH_2Cl_2 (4 mL) at room temperature. After stirring for 20 min, a solution of **L1** (10.3 mg, 0.04 mmol, 2 equiv.) in CH_2Cl_2 (6 mL) was added to the reaction mixture. After stirring for 30 min, the clear solution was layered with 30 mL of *n*-pentane. The Schlenk flask was kept in the dark at room temperature and **2a** precipitated as brown crystalline material after one week. The product was filtered, washed with *n*-pentane, and then dried in vacuo. Yield: 26 mg (61%). Recrystallization of **2a** from *o*-$C_6H_4F_2$ by layering with *n*-pentane affords brown crystals of **2b** in nearly qualitative yields. Method 2: to a stirring solution of **1** (20 mg, 0.004 mmol, 1 equiv.) in CH_2Cl_2 (3 mL) a solution of **L1** (1 mg, 0.004 mmol, 1 equiv.) in CH_2Cl_2 (2 mL) was added. After stirring for 20 min, the clear solution was layered with 30 mL of *n*-pentane. The Schlenk flask was kept in the dark at −30 °C and **2a** precipitated as brown crystalline material within one week. Yield 7 mg (44%). ^{1}H NMR (CD_2Cl_2, 25 °C): δ = 5.16 (s, 10H, H_{Cp}), 8.07 (br s, 4H, H_a), 9.14 (br s, 4H, H_b). ^{13}C{^{1}H} NMR (CD_2Cl_2, 25 °C): δ = 83.9 (s, C_{Cp}), 123.1 (s, C_a), 149.2 (s, C_b), 223.4 (s, C_{CO}). ^{19}F{^{1}H} NMR (CD_2Cl_2, 25 °C): δ = −75.6 (s, [TEF]$^-$). IR (KBr): $\tilde{\nu}$ = 3440 (br m), 2918 (w), 2850 (w), 1955 (s, CO), 1915 (s, CO), 1633 (m), 1604 (m), 1425 (w), 1386 (w), 1354 (m), 1303 (s), 1280 (s), 1243 (s), 1221 (s), 1167 (m), 974 (s),864 (m), 825 (m), 729 (s). ESI-MS (CH_2Cl_2): positive mode: *m/z* 1042.7 (100%, [{$Cp_2(CO)_4Mo_2Sb_2$}Ag($C_{16}H_8N_4$)]$^+$), 913.6 (38%, [{$Cp_2(CO)_4Mo_2Sb_2$}$_2$Ag$_2$($C_{16}H_8N_4$)]$^{2+}$), 1464.3 (6%, [{$Cp_2(CO)_4Mo_2Sb_2$}$_2$Ag]$^+$), 2795.1 (0.4%, [{{$Cp_2(CO)_4Mo_2Sb_2$}$_2$Ag$_2$($C_{16}H_8N_4$)}{Al{OC(CF_3)$_3$}$_4$}]$^+$). ESI-MS (CH_2Cl_2): negative mode: *m/z* 966.9 (100%, [Al{OC(CF_3)$_3$}$_4$]$^-$). Elemental analysis (%) calcd for $C_{46}H_{18}AgAlF_{36}Mo_2N_4O_8Sb_2$ (**2**) (2008.88 g·mol^{-1}): C 27.50, H 0.90, N 2.79; found: C 27.21, H 0.91, N 2.51.

*Synthesis of [(η^2-C)$_6$Ag$_4$(μ,$\eta^{1:1:1:1}$-L2)$_3$][TEF]$_4$ (**3**)*: A solution of Ag[TEF]·CH_2Cl_2 (23 mg, 0.02 mmol, 1 equiv.) in CH_2Cl_2 (3 mL) was added to a solution of **C** (26 mg, 0.04 mmol, 2 equiv.) in CH_2Cl_2 (3 mL) at room temperature. After stirring for 20 min, a solution of **L2** (6.5 mg, 0.04 mmol, 2 equiv.) in CH_2Cl_2 (2 mL) was added to the reaction mixture. After stirring for 30 min at room temperature, the clear solution was layered with 30 mL of *n*-pentane. The Schlenk flask was kept in the dark at −30 °C and **3** precipitated as orange crystalline material within two weeks. The product was filtered, washed with *n*-pentane, and then dried in vacuo. Yield: 20 mg (45%). ^{1}H NMR (CD_2Cl_2, 25 °C): δ = 5.19 (s, 60H, H_{Cp}), 7.73 (t, 6H, $^3J_{H,H}$ = 4.9 Hz, H_a), 9.13 (d, 12H, $^3J_{H,H}$ = 4.9 Hz, H_b). ^{13}C{^{1}H} NMR (CD_2Cl_2, 25 °C): δ = 83.6 (s, C_{Cp}), 120.7 (s, C_a), 159.4 (s, C_b), 223.6 (s, C_{CO}). ^{19}F{^{1}H} NMR (CD_2Cl_2, 25 °C): δ = −75.6 (s, [TEF]$^-$). IR (KBr): $\tilde{\nu}$ = 3441 (br m), 3128 (w), 2339 (w), 1946 (s, CO), 1905 (s, CO), 1562 (m), 1423 (m), 1410 (m), 1352 (s), 1301 (s), 1277 (s), 1241 (s), 1220 (s), 1167 (m), 1063 (w), 1007 (w), 974 (s), 836 (m), 827 (m), 761 (w), 728 (s), 686 (w), 653 (w). ESI-MS (CH_2Cl_2): positive mode: *m/z* 942.6 (100%, [{$Cp_2(CO)_4Mo_2Sb_2$}Ag($C_8H_6N_4$)]$^+$), 1464.3 (65%, [{$Cp_2(CO)_4Mo_2Sb_2$}$_2$Ag]$^+$, 1606.1 (0.3%, [{$Cp_2(CO)_4Mo_2Sb_2$}$_2$Ag$_2$Cl]$^+$), 2283.8 (0.1%, [{$Cp_2(CO)_4Mo_2Sb_2$}$_3$Ag$_2$Cl]$^+$), 2696.1 (0.1%, [{{$Cp_2(CO)_4Mo_2Sb_2$}$_2$Ag$_2$($C_8H_6N_4$)}{Al{OC(CF_3)$_3$}$_4$}]$^+$). ESI-MS (CH_2Cl_2): negative mode: *m/z* 966.9 (100%, [Al{OC(CF_3)$_3$}$_4$]$^-$). Elemental analysis (%) calcd for $C_{176}H_{86}Ag_4Al_4Cl_8F_{144}Mo_{12}N_{12}O_{40}Sb_{12}$ (**3**·4CH_2Cl_2) (9179.97 g·mol^{-1}): C 23.03, H 0.94, N 1.83; found: C 23.21, H 0.71, N 1.59.

*Synthesis of [(η^2-C)Ag(μ,$\eta^{1:1}$-L3)$_{1.5}$]$_n$[TEF]$_n$ (**4**)*: A solution of Ag[TEF]·CH_2Cl_2 (20 mg, 0.03 mmol, 1 equiv.) in CH_2Cl_2 (4 mL) was added to a solution of **C** (35 mg, 0.03 mmol, 1 equiv.) in CH_2Cl_2 (4 mL) at room temperature. After stirring for 20 min, a solution of **L3** (9.4 mg, 0.06 mmol, 2 equiv.) in CH_2Cl_2 (3 mL) was added to the reaction mixture. After stirring for 30 min at room temperature, the clear solution was layered with 30 mL of *n*-pentane. The Schlenk flask was kept in the dark at −30 °C and **4** precipitated as orange crystalline material within two weeks. The product was filtered, washed with *n*-pentane, and then dried in vacuo. Yield: 14 mg (23%). ^{1}H NMR (CD_2Cl_2, 25 °C): δ = 5.24 (s, 10H, H_{Cp}), 7.62 (dd, 6H, $^3J_{H,H}$ = 4.4 Hz, $^4J_{H,H}$ = 1.6 Hz, H_a), 8.71 (dd, 6H, $^3J_{H,H}$ = 4.4 Hz, $^4J_{H,H}$ = 1.6 Hz, H_b). ^{13}C{^{1}H} NMR (CD_2Cl_2, 25 °C): δ = 84.2 (s, C_{Cp}), 122.1 (s, C_a), 151.1 (s, C_b), 222.9 (s, C_{CO}). ^{19}F{^{1}H} NMR (CD_2Cl_2, 25 °C): δ = −75.6 (s, [TEF]$^-$). IR (KBr): $\tilde{\nu}$ = 3443 (br m), 3133 (w), 2919 (w), 2850 (w), 2341 (w), 1949 (s, CO), 1905 (s, CO), 1893 (s, CO), 1603 (m), 1537 (w), 1491 (w), 1424 (w), 1354 (m), 1303 (s), 1279 (s), 1243 (s), 1221 (s), 1164 (m), 1068 (w), 1003 (w), 974 (s), 828 (m), 807 (m), 757 (w), 729 (s), 623 (w). ESI-MS (CH_2Cl_2): positive mode: *m/z* 1464.3 (100%, [{$Cp_2(CO)_4Mo_2Sb_2$}$_2$Ag]$^+$), 940.6 (45%, [{$Cp_2(CO)_4Mo_2Sb_2$}Ag($C_{10}H_8N_2$)]$^+$). ESI-MS (CH_2Cl_2): negative mode: *m/z* 966.9 (100%, [Al{OC(CF_3)$_3$}$_4$]$^-$). Elemental analysis (%) calcd for $C_{45}H_{22}AgAlF_{36}Mo_2N_3O_8Sb_2$ (**4**) (1986.90 g·mol^{-1}): C 27.20, H 1.12, N 2.11; found: C 27.51, H 1.12, N 2.07.

*Synthesis of [($\eta^{2:1}$-C)$_4$Ag$_4$(μ,$\eta^{1:1}$-L4)$_4$]$_n$[TEF]$_{4n}$ (**5**)*: A solution of Ag[TEF]·CH_2Cl_2 (35 mg, 0.03 mmol, 1 equiv.) in CH_2Cl_2 (4 mL) was added to a solution of **C** (20 mg, 0.03 mmol, 1 equiv.) in CH_2Cl_2 (4 mL) at room temperature. After stirring for 20 min, a solution of **L4** (10.9 mg, 0.06 mmol, 2 equiv.) in CH_2Cl_2 (3 mL) was added to the reaction mixture. After stirring for 30 min at room temperature, the clear solution was layered with 30 mL of *n*-pentane. The Schlenk flask was kept in the dark at −30 °C and **5** precipitated as orange crystalline material within two weeks. The product was filtered, washed with *n*-pentane, and then dried in vacuo. Yield: 31 mg (53%). ^{1}H NMR (CD_2Cl_2, 25 °C): δ = 5.25 (s, 40H, H_{Cp}), 7.31 (s, 8H, H_a), 7.55 (dd, 16H, $^3J_{H,H}$ = 4.4 Hz, $^4J_{H,H}$ = 1.6 Hz, H_b), 8.54 (dd, 16H, $^3J_{H,H}$ = 4.4 Hz, $^4J_{H,H}$ = 1.6 Hz, H_c). ^{13}C{^{1}H} NMR (CD_2Cl_2, 25 °C): δ = 84.1 (s, C_{Cp}), 122.7 (s, C_b), 131.6 (s, C_a), 150.5 (s, C_c), 223.0 (s, C_{CO}). ^{19}F{^{1}H} NMR (CD_2Cl_2, 25 °C): δ = −75.6 (s, [TEF]$^-$). IR (KBr): $\tilde{\nu}$ = 3457 (br m), 2920 (w), 1953 (s, CO), 1914 (s, CO), 1607 (m), 1426 (w), 1386 (w), 1354 (m), 1303 (s), 1279 (s), 1244 (s), 1222 (s), 1167 (m), 1068 (w), 1010 (w), 974 (s), 826 (m), 757 (w), 729 (s). ESI-MS (CH_2Cl_2): positive mode: *m/z* 1464.3 (100%, [{$Cp_2(CO)_4Mo_2Sb_2$}$_2$Ag]$^+$), 968.7 (51%, [{$Cp_2(CO)_4Mo_2Sb_2$}$_2$Ag($C_{12}H_{10}N_2$)]$^+$). ESI-MS (CH_2Cl_2): negative mode: *m/z* 966.9 (100%, [Al{OC(CF_3)$_3$}$_4$]$^-$). Elemental analysis (%) calcd for $C_{168}H_{80}Ag_4Al_4F_{144}Mo_8N_8O_{32}Sb_8$ (**5**) (7739.37 g·mol^{-1}): C 26.07, H 1.04, N 1.45; found: C 25.93, H 0.68, N 1.30.

*Synthesis of [(η^2-C)$_2$Ag$_2$(μ,$\eta^{1:1}$-L5)$_3$]$_n$[TEF]$_{2n}$ (**6**)*: A solution of Ag[TEF]·CH_2Cl_2 (35 mg, 0.03 mmol, 1 equiv.) in CH_2Cl_2 (4 mL) was added to a solution of **C** (20 mg, 0.03 mmol, 1 equiv.) in CH_2Cl_2 (4 mL) at room temperature. After stirring for 20 min, a solution of **L5** (11.9 mg, 0.06 mmol, 2 equiv.)

in CH_2Cl_2 (3 mL) was added to the reaction mixture. After stirring for 30 min at room temperature, the clear solution was layered with 30 mL of *n*-pentane. The Schlenk flask was kept in the dark at −30 °C and **6** precipitated as orange crystalline material within two weeks. The product was filtered, washed with *n*-pentane, and then dried in vacuo. Yield: 39 mg (63 %). ^{1}H NMR (CD_2Cl_2, 25 °C): $\delta = 1.98$ (p, 6H, $^3J_{H,H} = 7.7$ Hz, H_a), 2.70 (t, 12H, $^3J_{H,H} = 7.7$ Hz, H_b), 5.23 (s, 20H, H_{Cp}), 7.22 (dd, 12H, $^3J_{H,H} = 4.3$ Hz, $^4J_{H,H} = 1.6$ Hz, H_c), 8.38 (dd, 12H, $^3J_{H,H} = 4.3$ Hz, $^4J_{H,H} = 1.6$ Hz, H_d). ^{13}C{^{1}H} NMR (CD_2Cl_2, 25 °C): $\delta = 30.7$ (s, C_a), 34.9 (s, C_b), 83.9 (s, C_{Cp}), 125.1 (s, C_c), 150.0 (s, C_d), 223.2 (s, C_{CO}). ^{19}F{^{1}H} NMR (CD_2Cl_2, 25 °C): $\delta = -75.6$ (s, $[TEF]^-$). IR (KBr): $\tilde{\nu} = 3434$ (br m), 3120 (w), 2949 (w), 2871 (w), 1950 (s, CO), 1904 (s, CO), 1610 (m), 1561 (w), 1501 (w), 1423 (m), 1393 (w), 1352 (m) 1301 (s), 1277 (s), 1241 (s), 1219 (s), 1167 (m), 1069 (w), 1009 (w), 974 (s), 828 (m), 755 (w), 728 (s), 607 (w). ESI-MS (CH_2Cl_2): positive mode: *m/z* 1464.3 (100 %, $[\{Cp_2(CO)_4Mo_2Sb_2\}_2Ag]^+$), 984.7 (34 %, $[\{Cp_2(CO)_4Mo_2Sb_2\}Ag(C_{13}H_{14}N_2)]^+$), 1606.1 (2 %, $[\{Cp_2(CO)_4Mo_2Sb_2\}_2Ag_2Cl]^+$). ESI-MS ($CH_2Cl_2$): negative mode: *m/z* 966.9 (100 %, $[Al\{OC(CF_3)_3\}_4]^-$). Elemental analysis (%) calcd for $C_{99}H_{62}Ag_2Al_2F_{72}Mo_4N_6O_{16}Sb_4$ (**6**) (4100.04 g·mol^{-1}): C 29.00, H 1.52, N 2.05; found: C 29.06, H 1.25, N 2.01.

DFT calculations: For all computations, the Gaussian 09 program package[33] was used throughout. Density functional theory (DFT) in the form of long-range corrected hybrid functional ωB97XD[34] featuring Grimme's dispersion correction[35] with a def2-SVP[36] basis set was employed. Solvent effects were modeled using a polarized continuous model[37] (PCM, $\varepsilon(CH_2Cl_2) = 8.93$). The geometries of the compounds were fully optimized and verified to be true minima on their respective potential energy surface.[38]

Crystallographic data: Deposition Numbers 2241559 (for **1**), 2241560 (for **2 a**), 2241561 (for **2 b**), 2241562 (for **3**), 2241563 (for **4**), 2241564 (for **5**), and 2241565 (for **6**) contain the supplementary crystallographic data for this paper. These data are provided free of charge by the joint Cambridge Crystallographic Data Centre and Fachinformationszentrum Karlsruhe Access Structures service.

Supporting Information

Additional references are cited in the Supporting Information.[39]

Acknowledgements

This work was supported by the Deutsche Forschungsgemeinschaft within the projects Sche 384/44-1 and Sche 384/42-1. Open Access funding enabled and organized by Projekt DEAL.

Conflict of Interests

The authors declare no conflict of interest.

Data Availability Statement

The data that support the findings of this study are available in the supplementary material of this article.

Keywords: antimony · N-donor ligands · organometallic–organic hybrid assemblies · silver · supramolecular coordination complexes

[1] a) Z. Y. Zhang, Z. Q. Zhao, L. W. Wu, S. Lu, S. L. Ling, G. P. Li, L. T. Xu, L. Z. Ma, Y. L. Hou, X. C. Wang, X. P. Li, G. He, K. Wang, B. Zou, M. M. Zhang, *J. Am. Chem. Soc.* **2020**, *142*, 2592–2600; b) T. L. Mako, J. M. Racicot, M. Levine, *Chem. Rev.* **2019**, *119*, 322–477; c) Y. Lu, H. N. Zhang, G. X. Jin, *Acc. Chem. Res.* **2018**, *51*, 2148–2158; d) M. M. Gan, J. Q. Liu, L. Zhan, Y. Y. Wang, F. E. Hahn, Y. F. Han, *Chem. Rev.* **2018**, *118*, 9587–9641; e) T. R. Cook, P. J. Stang, *Chem. Rev.* **2015**, *115*, 7001–7045; f) T. R. Cook, Y. R. Zheng, P. J. Stang, *Chem. Rev.* **2013**, *113*, 734–777; g) R. Chakrabarty, P. S. Mukherjee, P. J. Stang, *Chem. Rev.* **2011**, *111*, 6810–6918.

[2] a) X. X. Kong, Q. Q. Shen, T. T. Wan, K. Y. Li, F. G. Sun, H. L. Wu, *J. Chin. Chem. Soc.* **2022**, *69*, 540–548; b) K. Dammak, M. Porchia, M. D Franco, M. Zancato, H. Naili, V. Gandin, C. Marzano, *Molecules* **2020**, *25*, 5484; c) M. I. Rogovoy, D. G. Samsonenko, M. I. Rakhmanova, A. V. Artem'ev, *Inorg. Chim. Acta* **2019**, *489*, 19–26; d) J. M. Alderson, J. R. Corbin, J. M. Schomaker, *Acc. Chem. Res.* **2017**, *50*, 2147–2158; e) T. Zhang, H. Q. Huang, H. X. Mei, D. F. Wang, X. X. Wang, R. B. Huang, L. S. Zheng, *J. Mol. Struct.* **2015**, *1100*, 237–244; f) H. Y. Bai, J. Yang, B. Liu, J. F. Ma, W. Q. Kan, Y. Y. Liu, Y. Y. Liu, *CrystEngComm* **2011**, *13*, 5877–5884; g) R. G. Lin, J. H. K. Yip, *Inorg. Chem.* **2006**, *45*, 4423–4430.

[3] a) F. Prencipe, A. Zanfardino, M. Di Napoli, F. Rossi, S. D'Errico, G. Piccialli, G. F. Mangiatordi, M. Saviano, L. Ronga, M. Varcamonti, D. Tesauro, *Int. J. Mol. Sci.* **2021**, *22*, 2497; b) J. S. Jung, S. J. Ko, H. B. Lee, S. B. Lee, H. J. Kim, J. M. Oh, *Polymer* **2019**, *11*, 155; c) S. Joardar, S. Roy, S. Samanta, A. K. Dutta, *J. Chem. Sci.* **2015**, *127*, 1819–1826; d) S. Chernousova, M. Epple, *Angew. Chem. Int. Ed.* **2013**, *52*, 1636–1653.

[4] a) L. Xu, Y. Y. Wang, J. Huang, C. Y. Chen, Z. X. Wang, H. Xie, *Theranostics* **2020**, *10*, 8996–9031; b) S. S. Jeremiah, K. Miyakawa, T. Morita, Y. Yamaoka, A. Ryo, *Biochem. Biophys. Res. Commun.* **2020**, *533*, 195–200; c) X. X. Liang, S. X. Luan, Z. Q. Yin, M. He, C. L. He, L. Z. Yin, Y. F. Zou, Z. X. Yuan, L. X. Li, X. Song, C. Lv, W. Zhang, *Eur. J. Med. Chem.* **2018**, *157*, 62–80; d) S. Medici, M. Peana, G. Crisponi, V. M. Nurchi, J. I. Lachowicz, M. Remelli, M. A. Zoroddu, *Coord. Chem. Rev.* **2016**, *327*, 349–359; e) V. Incani, A. Omar, G. Prosperi-Porta, P. Nadworny, *Int. J. Antimicrob. Agents* **2015**, *45*, 586–593.

[5] a) S. M. Soliman, Y. N. Mabkhot, J. H. Albering, *J. Chem. Crystallogr.* **2020**, *50*, 52–61; b) P. Weis, C. Hettich, D. Kratzert, I. Krossing, *Eur. J. Inorg. Chem.* **2019**, *2019*, 1657–1668; c) R. Hamze, S. Y. Shi, S. C. Kapper, D. S. M. Ravinson, L. Estergreen, M. C. Jung, A. C. Tadle, R. Haiges, P. I. Djurovich, J. L. Peltier, R. Jazzar, G. Bertrand, S. E. Bradforth, M. E. Thompson, *J. Am. Chem. Soc.* **2019**, *141*, 10118–10118; d) S. Evariste, A. M. Khalil, M. E. Moussa, A. K. W. Chan, E. Y. H. Hong, H. L. Wong, B. Le Guennic, G. Calvez, K. Costuas, V. W. W. Yam, C. Lescop, *J. Am. Chem. Soc.* **2018**, *140*, 12521–12526; e) D. Yadav, R. K. Siwatch, G. Mukherjee, G. Rajaraman, S. Nagendran, *Inorg. Chem.* **2014**, *53*, 10054–10059; f) A. Serpe, F. Artizzu, L. Marchio, M. L. Mercuri, L. Pilia, P. Deplano, *Cryst. Growth Des.* **2011**, *11*, 1278–1286; g) A. G. Young, L. R. Hanton, *Coord. Chem. Rev.* **2008**, *252*, 1346–1386; h) F. Hung-Low, K. K. Klausmeyer, *Inorg. Chim. Acta* **2008**, *361*, 1298–1310; i) A. N. Khlobystov, A. J. Blake, N. R. Champness, D. A. Lemenovskii, A. G. Majouga, N. V. Zyk, M. Schroder, *Coord. Chem. Rev.* **2001**, *222*, 155–192; j) F. A. Cotton, E. V. Dikarev, M. A. Petrukhina, *Angew. Chem. Int. Ed.* **2001**, *40*, 1521–1523.

[6] a) F. L. Zhang, L. Tian, L. F. Qin, J. Q. Chen, Z. J. Li, X. H. Ren, Z. G. Gu, *Polyhedron* **2016**, *104*, 9–16; b) S. Welsch, C. Lescop, M. Scheer, R. Reau, *Inorg. Chem.* **2008**, *47*, 8592–8594; c) Z. P. Deng, L. N. Zhu, S. Gao, L. H. Huo, S. W. Ng, *Cryst. Growth Des.* **2008**, *8*, 3277–3284; d) B. L. Schottel, H. T. Chifotides, M. Shatruk, A. Chouai, L. M. Perez, J. Bacsa, K. R. Dunbar, *J. Am. Chem. Soc.* **2006**, *128*, 5895–5912.

[7] a) J. M. Hao, B. Y. Yu, K. Van Hecke, G. H. Cui, *CrystEngComm* **2015**, *17*, 2279–2293; b) J. Z. Gu, Y. H. Cui, J. Wu, A. M. Kirillov, *RSC Adv.* **2015**, *5*, 78889–78901; c) G. Dura, M. C. Carrion, F. A. Jalon, B. R. Manzano, A. M. Rodriguez, K. Mereiter, *Cryst. Growth Des.* **2015**, *15*, 3321–3331; d) G. Kumar, R. Gupta, *Chem. Soc. Rev.* **2013**, *42*, 9403–9453; e) B. Nohra, Y. Yao, C. Lescop, R. Reau, *Angew. Chem. Int. Ed.* **2007**, *46*, 8242–8245; f) F. A. Cotton, C. Lin, C. A. Murillo, *Acc. Chem. Res.* **2001**, *34*, 759–771; g) M. J. Irwin, J. J. Vittal, G. P. A. Yap, R. J. Puddephatt, *J. Am. Chem. Soc.* **1996**, *118*, 13101–13102.

[8] a) M. E. Moussa, E. Peresypkina, A. V. Virovets, D. Venus, G. Balazs, M. Scheer, *CrystEngComm* **2018**, *20*, 7417–7422; b) H. N. Wang, G. G. Shan,

H. B. Li, X. L. Wang, H. T. Cao, Z. M. Su, *CrystEngComm* **2014**, *16*, 2754–2759; c) B. J. Holliday, C. A. Mirkin, *Angew. Chem. Int. Ed.* **2001**, *40*, 2022–2043; d) M. Fujita, K. Umemoto, M. Yoshizawa, N. Fujita, T. Kusukawa, K. Biradha, *Chem. Commun.* **2001**, 509–518.

[9] a) K. Skoch, I. Cisarova, P. Stepnicka, *Inorg. Chem. Commun.* **2017**, *84*, 234–236; b) K. Skoch, I. Cisarova, J. Schulz, U. Siemeling, P. Stepnicka, *Dalton Trans.* **2017**, *46*, 10339–10354; c) K. Skoch, F. Uhlik, I. Cisarova, P. Stepnicka, *Dalton Trans.* **2016**, *45*, 10655–10671.

[10] a) C. Heindl, E. V. Peresypkina, D. Ludeker, G. Brunklaus, A. V. Virovets, M. Scheer, *Chem. Eur. J.* **2016**, *22*, 2599–2604; b) F. Dielmann, E. V. Peresypkina, B. Kramer, F. Hastreiter, B. P. Johnson, M. Zabel, C. Heindl, M. Scheer, *Angew. Chem. Int. Ed.* **2016**, *55*, 14833–14837; c) M. Fleischmann, S. Welsch, E. V. Peresypkina, A. V. Virovets, M. Scheer, *Chem. Eur. J.* **2015**, *21*, 14332–14336; d) L. J. Gregoriades, B. K. Wegley, M. Sierka, E. Brunner, C. Groger, E. V. Peresypkina, A. V. Virovets, M. Zabel, M. Scheer, *Chem. Asian J.* **2009**, *4*, 1578–1587; e) M. Scheer, L. J. Gregoriades, M. Zabel, J. Bai, I. Krossing, G. Brunklaus, H. Eckert, *Chem. Eur. J.* **2008**, *14*, 282–295; f) J. F. Bai, A. V. Virovets, M. Scheer, *Angew. Chem. Int. Ed.* **2002**, *41*, 1737–1740.

[11] a) M. E. Moussa, M. Fleischmann, G. Balazs, A. V. Virovets, E. Peresypkina, P. A. Shelyganov, M. Seidl, S. Reichl, M. Scheer, *Chem. Eur. J.* **2021**, *27*, 9742–9747; b) M. E. Moussa, J. Schiller, E. Peresypkina, M. Seidl, G. Balazs, P. Shelyganov, M. Scheer, *Chem. Eur. J.* **2020**, *26*, 14315–14319; c) L. J. Gregoriades, H. Krauss, J. Wachter, A. V. Virovets, M. Sierka, M. Scheer, *Angew. Chem. Int. Ed.* **2006**, *45*, 4189–4192.

[12] a) M. E. Moussa, P. A. Shelyganov, M. Seidl, E. Peresypkina, N. Berg, R. M. Gschwind, G. Balazs, J. Schiller, M. Scheer, *Chem. Eur. J.* **2021**, *27*, 5028–5034; b) J. Schiller, A. Schreiner, M. Seidl, G. Balazs, M. Scheer, *Chem. Eur. J.* **2020**, *26*, 14570–14574; c) M. E. Moussa, M. Fleischmann, E. V. Peresypkina, L. Dutsch, M. Seidl, G. Balazs, M. Scheer, *Eur. J. Inorg. Chem.* **2017**, *2017*, 3222–3226.

[13] a) E. Peresypkina, K. Grill, B. Hiltl, A. V. Virovets, W. Kremer, J. Hilgert, W. Tremel, M. Scheer, *Angew. Chem. Int. Ed.* **2021**, *60*, 12132–12142; b) E. Peresypkina, C. Heindl, A. Virovets, H. Brake, E. Madl, M. Scheer, *Chem. Eur. J.* **2018**, *24*, 2503–2508; c) C. Heindl, E. Peresypkina, A. V. Virovets, I. S. Bushmarinov, M. G. Medvedev, B. Kramer, B. Dittrich, M. Scheer, *Angew. Chem. Int. Ed.* **2017**, *56*, 13237–13243; d) F. Dielmann, C. Heindl, F. Hastreiter, E. V. Peresypkina, A. V. Virovets, R. M. Gschwind, M. Scheer, *Angew. Chem. Int. Ed.* **2014**, *53*, 13605–13608; e) M. Scheer, A. Schindler, R. Merkle, B. P. Johnson, M. Linseis, R. Winter, C. E. Anson, A. V. Virovets, *J. Am. Chem. Soc.* **2007**, *129*, 13386–13387; f) J. F. Bai, A. V. Virovets, M. Scheer, *Science* **2003**, *300*, 781–783.

[14] S. Welsch, C. Groger, M. Sierka, M. Scheer, *Angew. Chem. Int. Ed.* **2011**, *50*, 1435–1438.

[15] H. Brake, E. Peresypkina, C. Heindl, A. V. Virovets, W. Kremer, M. Scheer, *Chem. Sci.* **2019**, *10*, 2940–2944.

[16] a) E. Peresypkina, M. Bielmeier, A. Virovets, M. Scheer, *Chem. Sci.* **2020**, *11*, 9067–9071; b) M. Fleischmann, S. Welsch, H. Krauss, M. Schmidt, M. Bodensteiner, E. V. Peresypkina, M. Sierka, C. Groger, M. Scheer, *Chem. Eur. J.* **2014**, *20*, 3759–3768; c) H. Krauss, G. Balazs, M. Bodensteiner, M. Scheer, *Chem. Sci.* **2010**, *1*, 337–342; d) M. Scheer, L. J. Gregoriades, A. V. Virovets, W. Kunz, R. Neueder, I. Krossing, *Angew. Chem. Int. Ed.* **2006**, *45*, 5689–5693.

[17] a) M. E. Moussa, J. Schiller, M. Seidl, P. A. Shelyganov, M. Scheer, *New J. Chem.* **2021**, *45*, 1800–1804; b) M. E. Moussa, S. Welsch, M. Lochner, E. V. Peresypkina, A. V. Virovets, M. Scheer, *Eur. J. Inorg. Chem.* **2018**, *2018*, 2689–2694; c) M. E. Moussa, B. Attenberger, E. V. Peresypkina, M. Scheer, *Dalton Trans.* **2018**, *47*, 1014–1017; d) M. E. Moussa, M. Seidl, G. Balazs, M. Zabel, A. V. Virovets, B. Attenberger, A. Schreiner, M. Scheer, *Chem. Eur. J.* **2017**, *23*, 16199–16203; e) M. E. Moussa, B. Attenberger, M. Seidl, A. Schreiner, M. Scheer, *Eur. J. Inorg. Chem.* **2017**, *2017*, 5616–5620; f) M. E. Moussa, B. Attenberger, E. V. Peresypkina, M. Fleischmann, G. Balazs, M. Scheer, *Chem. Commun.* **2016**, *52*, 10004–10007; g) B. Attenberger, E. V. Peresypkina, M. Scheer, *Inorg. Chem.* **2015**, *54*, 7021–7029; h) B. Attenberger, S. Welsch, M. Zabel, E. Peresypkina, M. Scheer, *Angew. Chem. Int. Ed.* **2011**, *50*, 11516–11519.

[18] O. J. Scherer, H. Sitzmann, G. Wolmershäuser, *J. Organomet. Chem.* **1984**, *268*, C9-C12.

[19] P. J. Sullivan, A. L. Rheingold, *Organometallics* **1982**, *1*, 1547–1549.

[20] a) P. A. Shelyganov, M. Elsayed Moussa, M. Seidl, M. Scheer, *Angew. Chem. Int. Ed.* **2022**, *61*, e202215650; b) H. V. Ly, M. Parvez, R. Roesler, *Inorg. Chem.* **2006**, *45*, 345–351.

[21] a) B. W. Skelton, A. H. White, *CSD Communication (Private Communication)* **2018**; b) C. N. Banti, C. Papatriantafyllopoulou, M. Manoli, A. J. Tasiopoulos, S. K. Hadjikakou, *Inorg. Chem.* **2016**, *55*, 8681–8696; c) C. Di Nicola, Effendy, F. Marchetti, C. Pettinari, B. W. Skelton, A. H. White, *Inorg. Chim. Acta* **2007**, *360*, 1433–1450; d) Effendy, F. Marchetti, C. Pettinari, R. Pettinari, M. Ricciutelli, B. W. Skelton, A. H. White, *Inorg. Chem.* **2004**, *43*, 2157–2165; e) A. Cingolani Effendy, M. Pellei, C. Pettinari, C. Santini, B. W. Skelton, A. H. White, *Inorg. Chem.* **2002**, *41*, 6633–6645; f) K. V. Domasevitch, E. G. Petkova, A. Y. Nazarenko, V. V. Ponomareva, J. Sieler, N. K. Dalley, E. B. Rusanov, *Z. Naturforsch. B* **1999**, *54*, 904–912; g) Effendy, J. D. Kildea, A. H. White, *Aust. J. Chem.* **1997**, *50*, 587–604.

[22] The species with the fromula $[(\eta^2\text{-}\mathbf{C})\mathrm{Ag}(\mu,\eta^{1:1:1:1}\text{-}\mathbf{L1})]^+$ was used as a model compound for **2** (namely **2a**). For more details see the Supporting Information.

[23] C. R. Groom, I. J. Bruno, M. P. Lightfoot, S. C. Ward, *Acta Crystallogr. B Struct. Sci. Cryst. Eng. Mater.* **2016**, *72*, 171–179.

[24] Calculated as the diagonal distances between Ag^I ions minus the doubled ionic radius of Ag^I ions for the coordination number 4 (1.14 Å).

[25] H. Schmidbaur, A. Schier, *Angew. Chem. Int. Ed.* **2015**, *54*, 746–784.

[26] E. G. Hohenstein, C. D. Sherrill, *J. Phys. Chem. A* **2009**, *113*, 878–886.

[27] To model organometallic–organic nodes of CPs **4**–**6** each pyridine function of the ditopic linkers **L3**-**L5** was replaced with pyridine molecule (**py**). As a result, model systems $[(\eta^2\text{-}\mathbf{C})\mathrm{Ag}(\mathbf{py})_3]^+$ (for **4**, **6**) and $[(\eta^{2:1}\text{-}\mathbf{C})_2\mathrm{Ag}_2(\mathbf{py})_4]^{2+}$ (for **5**) were obtained.

[28] To reveal the coordination geometry that best describes the environment of the Ag^I centers, the proximity (root-mean-square displacement of atomic coordinates) to the corresponding symmetry groups was calculated. For more information see the Supporting Information.

[29] a) M. Fleischmann, J. S. Jones, G. Balazs, F. P. Gabbai, M. Scheer, *Dalton Trans.* **2016**, *45*, 13742–13749; b) J. R. Harper, A. L. Rheingold, *J. Organomet. Chem.* **1990**, *390*, C36-C38.

[30] L. Dutsch, C. Riesinger, G. Balazs, M. Scheer, *Chem. Eur. J.* **2021**, *27*, 8804–8810.

[31] I. Krossing, *Chem. Eur. J.* **2001**, *7*, 490–502.

[32] T. Brietzke, W. Mickler, A. Kelling, H. J. Holdt, *Dalton Trans.* **2012**, *41*, 2788–2797.

[33] *Gaussian 09, Revision E.01*, M. J. Frisch, G. W. Trucks, H. B. Schlegel, G. E. Scuseria, M. A. Robb, J. R. Cheeseman, G. Scalmani, V. Barone, B. Mennucci, G. A. Petersson, H. Nakatsuji, M. Caricato, X. Li, H. P. Hratchian, A. F. Izmaylov, J. Bloino, G. Zheng, J. L. Sonnenberg, M. Hada, M. Ehara, K. Toyota, R. Fukuda, J. Hasegawa, M. Ishida, T. Nakajima, Y. Honda, O. Kitao, H. Nakai, T. Vreven, J. A. Montgomery, Jr., J. E. Peralta, F. Ogliaro, M. Bearpark, J. J. Heyd, E. Brothers, K. N. Kudin, V. N. Staroverov, T. Keith, R. Kobayashi, J. Normand, K. Raghavachari, A. Rendell, J. C. Burant, S. S. Iyengar, J. Tomasi, M. Cossi, N. Rega, J. M. Millam, M. Klene, J. E. Knox, J. B. Cross, V. Bakken, C. Adamo, J. Jaramillo, R. Gomperts, R. E. Stratmann, O. Yazyev, A. J. Austin, R. Cammi, C. Pomelli, J. W. Ochterski, R. L. Martin, K. Morokuma, V. G. Zakrzewski, G. A. Voth, P. Salvador, J. J. Dannenberg, S. Dapprich, A. D. Daniels, O. Farkas, J. B. Foresman, J. V. Ortiz, J. Cioslowski, D. J. Fox, Gaussian, Inc., Wallingford CT, **2013**.

[34] J. D. Chai, M. Head-Gordon, *Phys. Chem. Chem. Phys.* **2008**, *10*, 6615–6620.

[35] S. Grimme, *J. Comput. Chem.* **2006**, *27*, 1787–1799.

[36] F. Weigend, R. Ahlrichs, *Phys. Chem. Chem. Phys.* **2005**, *7*, 3297–3305.

[37] G. Scalmani, M. J. Frisch, *J. Chem. Phys.* **2010**, *132*, 114110.

[38] Compound $[(\eta^2\text{-}\mathbf{C})\mathrm{Ag}(\mathbf{py})_3]^+$ ($\mathbf{py} = C_5H_5N$) shows one imaginary frequency ($-8\ cm^{-1}$). This small value was attributed to the little deformation of the structures due to flat contour of energy minimum. This compound was therefore also considered as minima.

[39] a) G. M. Sheldrick, *Acta Crystallogr. Sect. C Struct. Chem.* **2015**, *71*, 3–8; b) G. M. Sheldrick, *Acta Crystallogr. Sect. A Found. Adv.* **2015**, *71*, 3–8; c) O. V. Dolomanov, L. J. Bourhis, R. J. Gildea, J. A. K. Howard, H. Puschmann, *J. Appl. Crystallogr.* **2009**, *42*, 339–341; d) B. Metz, H. Stoll, M. Dolg, *J. Chem. Phys.* **2000**, *113*, 2563–2569; e) D. Andrae, U. Haussermann, M. Dolg, H. Stoll, H. Preuss, *Theor. Chim. Acta* **1990**, *77*, 123–141; f) G. A. Zhurko, D. A. Zhurko, *ChemCraft, Tool for Treatment of the Chemical Data*, http://www.chemcraftprog.com; g) CrysAlisPro Software System, Rigaku Oxford Diffraction (2018-2020).

Manuscript received: February 23, 2023
Accepted manuscript online: April 21, 2023
Version of record online: ■■, ■■

RESEARCH ARTICLE

The first mixed-ligand self-assembly reactions of the organometallic diantimony complex $[(Cp)_2Mo_2(CO)_4(\mu,\eta^2\text{-}Sb_2)]$ (**C**) with Ag[TEF] ([TEF] = [Al{OC$(CF_3)_3\}_4$]) in the presence of various N-donor molecules are presented. Depending on the organic linker, these reactions lead to the formation of two 0D, three 1D or one 2D novel hybrid organometallic–organic supramolecular aggregates. One of the polymeric assemblies represents a unique compound incorporating both Sb- and N-donor ligands as connectors for metal ions.

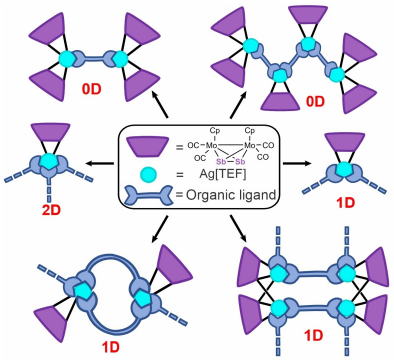

*P. A. Shelyganov, Dr. M. Elsayed Moussa, Dr. M. Seidl, Prof. Dr. M. Scheer**